Dependence of DC Characteristics of CNT MOSFETs on Bandstructure Models

Siyuranga O. Koswatta, Neophytos Neophytou, *Student Member, IEEE*, Diego Kienle, Gianluca Fiori, and Mark S. Lundstrom, *Fellow, IEEE*

Abstract—Since their discovery in the early 1990s, the interest in carbon nanotube (CNT) electronics has exploded. One main factor that controls the device performance of CNT field-effect transistors (CNT MOSFETs) is the electronic structure of the nanotube. In this paper we use three different bandstructure models: 1) extended Hückel theory (EHT); 2) orthogonal p_z tight-binding (OTB); and 3) parabolic effective mass model (EFM) to investigate the bandstructure effects on the device characteristics of a CNT MOSFET using semiclassical and quantum treatments of transport. We find that, after proper calibration, the OTB model is essentially identical to the EHT over the energy range of interest. We also find that an even simpler parabolic EFM facilitates CNT MOSFET simulations within practically applied bias ranges.

Index Terms—Bandstructure, Boltzmann transport, carbon nanotube (CNT) field-effect transistors (CNT MOSFETs), nonequilibrium Green's function (NEGF), semiclassical.

I. INTRODUCTION

DURING THE last few years, it has been realized that a qualitative and particularly quantitative understanding of nanoscale devices demand a rigorous treatment of electronic structure and transport in order to properly treat effects due to structure relaxation, quantum confinement, and scattering. Effective mass models (EFMs) have been commonly used to study conventional devices and have also been applied to new channel materials such as carbon nanotubes (CNTs) and silicon nanowires [1]–[7]. However, these models often carry free parameters that need to be adjusted using more rigorous calculations in order to reproduce the physical bandstructure of the material, at least in the energy range of interest. Empirical models are very appealing, since the atomistic features of the material can be effectively captured by a few parameters such as the effective mass tensor and the bandgap. One of the main drawbacks of these simplified bandstructure models, however, is their limited range of validity.

On the other hand, tight-binding approaches for electronic structure calculations are very popular due to their computational efficiency, improved range of validity, and the atomistic nature of the treatment [8], [9]. In the case of CNTs, the orthogonal p_z tight-binding (OTB) treatment has been widely used in electronic structure calculations [10]. Even though useful in describing electronic bands of CNTs with diameter $d \geq 1$ nm, a simple p_z orbital model fails to accurately capture the curvature induced effects in smaller diameter CNTs ($d < 1$ nm). A more rigorous calculation that can accurately capture the curvature induced effects in CNTs is a treatment based on the extended Hückel theory (EHT) [11], [12]. Nevertheless, the range of validity of simpler bandstructure models such as EFM and OTB can be extended by calibrating them against more advanced calculations as EHT. For example, in the case of silicon nanowires the validity of the parabolic effective mass approximation has been extended to wire diameters down to $d \approx 1$ nm by recalibrating the effective masses using $sp^3s^*d^5$ tight-binding calculations [13].

In this work we examine the validity of the OTB and the parabolic EFM models for the simulation of semiconducting zigzag CNT MOSFETs by comparing to the results obtained from the EHT treatment. The limitations and the range of validity of the parabolic EFM are examined. Calibration of the empirical fitting parameters of OTB and parabolic EFM models in order to extend their validity for smaller diameter CNTs is also presented. The dependence of current-voltage (*I–V*) characteristics on the bandstructure models is examined using both semiclassical and quantum transport simulation. For the case of semiclassical transport the Boltzmann transport equation (BTE) is solved in the ballistic limit [14]. We then perform a quantum transport simulation using the nonequilibrium Green's functions (NEGF) formalism [15], [16]. We find that both semiclassical and quantum transport calculations give similar results. We show that the *I–V* characteristics using a parabolic EFM approximation for the conduction band compares well with the more rigorous bandstructure model over a wide range of applied biases.

II. BANDSTRUCTURE MODELS

The first model we consider for the $E - k$ dispersion is based on EHT [11], where a Slater–Koster tight-binding scheme is employed [17], whose main features are summarized here. The main difference between a common OTB approach [10] and EHT is that the orbital basis functions $\phi_\mu(r)$ are nonorthogonal in the latter, i.e., the overlap matrix $S_{\mu\nu} \neq \delta_{\mu\nu}$ where $\delta_{\mu\nu}$ is the

Kronecker's delta function. In contrast to OTB, the EHT-basis functions are known explicitly, so that the matrix elements of the Hamiltonian H are calculated by [11], [12]

$$H_{\mu\mu} = E_{\mu\mu},$$
$$H_{\mu\nu} = 0.5 K_{eht} S_{\mu\nu} (H_{\mu\mu} + H_{\nu\nu}), \quad S_{\mu\nu} = \int d^3 r \phi_\mu^*(r) \phi_\nu(r)$$

where the onsite energy $E_{\mu\mu}$ as well as K_{eht} are fit parameters. As described in more detail in [12] and [17], the matrix elements $S_{\mu\nu}, H_{\mu\nu}$ are used to calculate the k-dependent matrix elements

$$H_{i,j}(k) = \sum_{j',m'} e^{ik(R_{i0} - R_{j'm'})} H_{i0,j'm'}$$
$$S_{i,j}(k) = \sum_{j',m'} e^{ik(R_{i0} - R_{j'm'})} S_{i0,j'm'}$$

between all atoms i and j' that are equivalent to the unit cell atoms i and j. Here, k is the wavevector within the first Brillouin zone. The band dispersion $E - k$ is then determined by solving for each k the generalized eigenvalue problem $H(k)A(k) = E(k)S(k)A(k)$, where $A(k)$ denotes the eigenvector. The EHT parameters used here have been optimized and benchmarked to reproduce the bulk bandstructure of a two-dimensional (2-D) graphene sheet calculated within density functional theory using the general gradient approximation [18]. Afterwards, employing these parameters in EHT calculation, the bandgaps for different CNT chiralities have been compared to the gaps obtained from surface tunneling spectroscopy (STS) experiments reported in [19], and find a good quantitative match [12]. Since the electronic dispersion determined from EHT does not require any further parameter calibration in order to quantitatively match the $E - k$'s of three-dimensional (3-D) CNT structures, the EHT-model serves in this work as the reference to describe the lowest conduction band.

As the second model, we use a nearest neighbor OTB description with a single p_z orbital for each atom. This model is based on the dispersion of a planar 2-D graphene sheet where the one-dimensional (1-D) dispersion of the CNT is calculated by means of a zone-folding scheme [10]. Within the nearest neighbor approximation, the OTB band dispersion can be calculated analytically, and for a zigzag nanotube with chirality $(n, 0)$ it is given by [10]

$$E(k) = \pm t \sqrt{1 + 4\cos\left(\frac{3ka_{cc}}{2}\right)\cos\left(\frac{\nu\pi}{n}\right) + 4\cos\left(\frac{\nu\pi}{n}\right)} \tag{1}$$

where a_{cc} is the carbon–carbon bonding distance, n is the tube chirality, ν is the subband index, and t is the nearest neighbor hopping parameter. The wavevector k is taken within the first Brillouin zone with values $-\pi/T < k < \pi/T$, where T denotes the 1-D translation vector along the transport direction. A typical value for t is 2.7 eV, but is generally a fitting parameter adjusted to match STS data close to the Fermi energy and is allowed to vary from 2.5 to 3.2 eV [10]. In this work we follow

t parameters used in calibrating OTB and parabolic EFM models to EHT			
Chirality *(n,0)*	Diameter *(nm)*	Bandgap *(eV)*	*t* *(eV)*
(13,0)	1.03	0.71	2.62
(10,0)	0.79	0.91	2.59
(7,0)	0.56	1.21	2.44

the same philosophy and consider t as a free parameter, which is adjusted such that the same value for the bandgap as provided by the EHT reference is obtained.

The third model is a parabolic effective mass (EFM) description of the conduction band which is based on the exact analytical $E - k$ expression for the OTB model, i.e., (1). The dispersion of the conduction band within the parabolic EFM model is obtained by a second-order Taylor expansion of (1) around the Γ-point $(k = 0)$ of the 1-D Brillouin zone, and is given by

$$E(k) = \pm\left(E_0 + \frac{\hbar^2}{2m^*}k^2\right), \quad E_0 = \frac{a_{cc}t}{d}, \quad m^* = \frac{4\hbar^2}{9ta_{cc}d} \tag{2}$$

where m^* is the effective mass, d is the tube diameter, and, E_0 is the onsite energy. It is common to set $E_0 = 0.0$ eV, which means that the Fermi level (midgap in the case of intrinsic semiconductors) is at zero energy.

III. RESULTS AND DISCUSSION

As mentioned earlier, in comparing the aforementioned bandstructure models, the EHT results are treated as the reference calculation. The parameter t in (1) and (2) is considered a fitting parameter and adjusted such that the CNT bandgap determined by OTB and parabolic EFM models agree with that given by EHT. Afterwards a comparison of the shape of the first conduction band can be made in order to ascertain the energy range of validity of the $E - k$ dispersions given by OTB and parabolic EFM models. Here, it should be noted that we concentrate on the first conduction/valence bands, since they are the dominant subbands participating in electrical transport in smaller diameter CNTs ($d \sim$ few nanometers). We have studied the electronic dispersion of three zigzag semiconducting CNTs: (13,0), (10,0), and (7,0). The t parameters required in matching the bandgaps between OTB and parabolic EFM with EHT are reported in Table I. The $E-k$ of the first conduction band determined by the three bandstructure models for the case of (13,0) CNT is shown in Fig. 1. We observe similar $E-k$ relations for (10,0) and (7,0) CNTs. It should be noted that the OTB dispersion agrees very well with that of EHT for energies up to several eV's. However, the parabolic EFM approximation is valid only up to few hundred meV's, and the band nonparabolicity becomes important at higher energies. In the case of the (13,0) tube, parabolic $E-k$ diverges from OTB and EHT for energies $E \geq 200$ meV. Nevertheless, it can be concluded that with proper calibration,
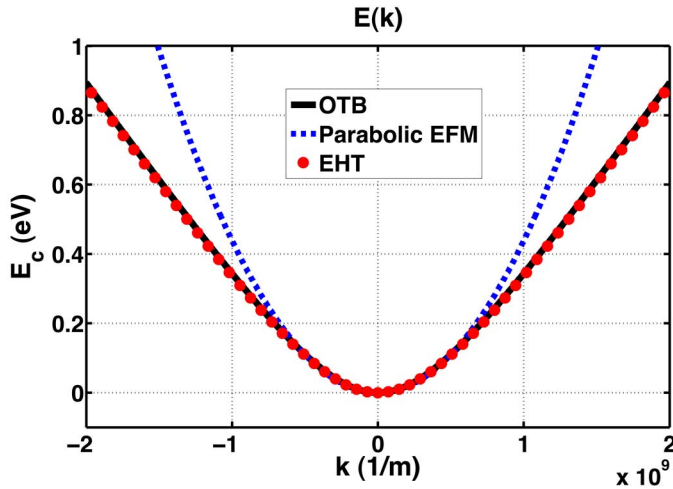
Fig 1. Band dispersion of the first conduction band for a (13,0) CNT using different bandstructure models. Circles: EHT, solid: OTB, (1), and dashed: parabolic EFM model (2). Parabolic EFM model agrees well with the other two up to $E \approx 200$ meV. (Color version available online at http://ieeexplore.ieee.org.)
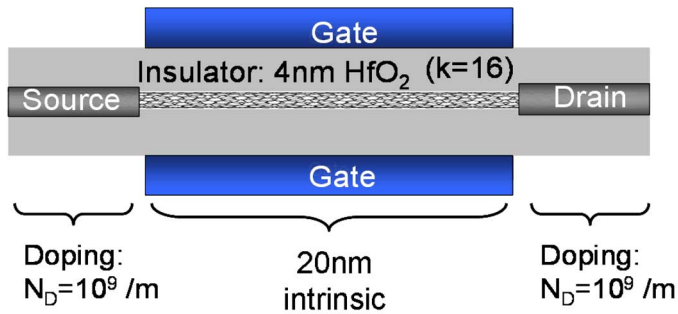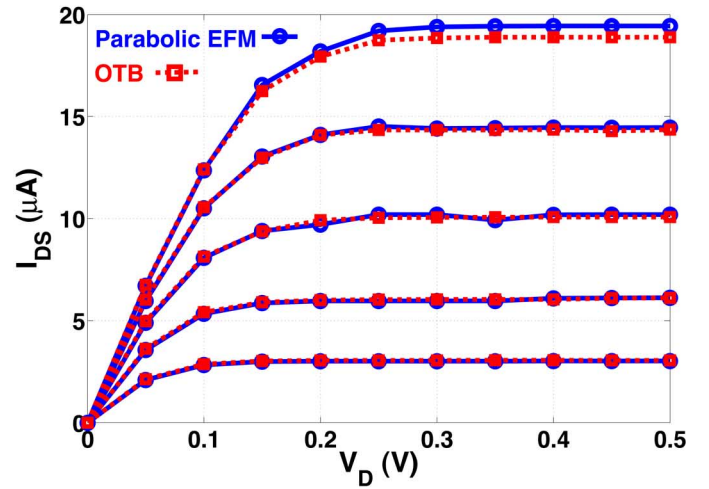

Fig. 2. Sketch of the device structure for the CNT MOSFET using a cylindrical gate to ensure full gate control. The channel length is $L = 20$ nm and the doping concentration of the 40-nm-long source/drain region is $10^9 m^{-1}$. The oxide is HfO$_2$ with a dielectric constant of $\kappa = 16$ and oxide thickness $t_{\text{ox}} = 4$ nm. (Color version available online at http://ieeexplore.ieee.org.)
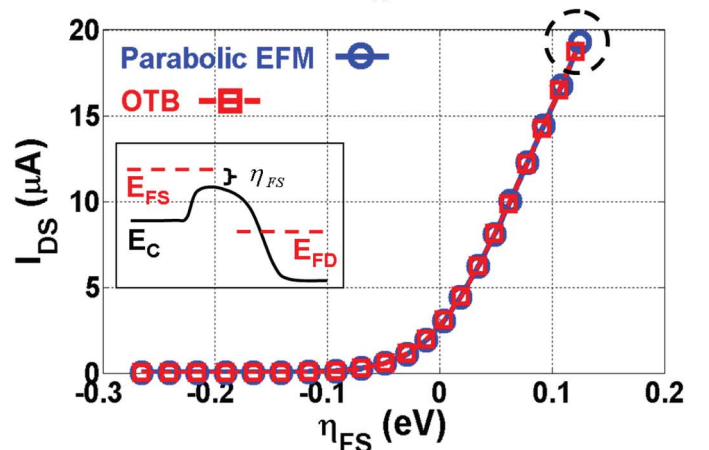
OTB and EHT bandstructures agree very well over a wide energy range that is important for CNT MOSFET operation.

In order to examine the impact of band nonparabolicity on semiclassical electron transport, we employ BTE simulations [14], to compare the I–V characteristics of CNT MOSFETs computed with different band dispersion models. The BTE treatment provides a semiclassical description that captures realistic 3-D electrostatic effects [14]. Because we have shown earlier that the bandstructure given by OTB and EHT match very well, here we only compare the I–V's between OTB and the parabolic EFM model. The CNT MOSFET structure employed in this study, shown in Fig. 2, is composed of a cylindrical wrap around gate with high-k HfO$_2$ gate oxide of $t_{\text{ox}} = 4$ nm. The source/drain regions are n-type doped ($N_{S/D} = 10^7$ cm^{-1}) and the channel region is undoped.

Simulated $I_{\text{DS}} - V_{\text{DS}}$ and $I_{\text{DS}} - \eta_{\text{FS}}$ results for the (13,0) tube with OTB and parabolic EFM bandstructures are shown in Fig. 3(a) and 3(b), respectively. Here, $\eta_{\text{FS}} = E_{\text{FS}} - E_{\text{C-TOB}}$ where E_{FS} is the source Fermi energy and $E_{\text{C-TOB}}$ is the energy of the top of the channel barrier [see inset of Fig. 3(b)]. From Fig. 3(a) it is seen that the output characteristics of the CNT MOSFET can be well captured by the parabolic EFM model for the voltage bias range of interest ($V_{\text{GS}} = 0.5$ V).

(a)

(b)

Fig. 3. I–V results for the (13,0) CNT MOSFET using semiclassical BTE simulation: solid circles—parabolic EFM and dashed squares—OTB. (a) $I_{\text{DS}} - V_{\text{DS}}$ for V_{GS} varied from 0.3 to 0.5 V in steps of 0.05 V. (b) $I_{\text{DS}} - \eta_{\text{FS}}$ results with $V_{\text{DS}} = 0.5$ V and V_{GS} varied from 0.0 to 0.5 V in steps of 0.025 V. The inset shows the conduction band profile with respect to source/drain Fermi levels in the ON-state. (Color version available online at http://ieeexplore.ieee.org.)

However, the discrepancy in $I_{\text{DS}} - V_{\text{DS}}$ for the two bandstructure models increases at large gate voltages as the band nonparabolicity becomes more influential on the I–V characteristics. It is important to note that in 1-D semiclassical transport, the device current (I_{DS}) does not directly depend on the bandstructure model.[1] The effect of bandstructure enters when the top of the channel barrier position ($E_{\text{C-TOB}}$) is determined through the self-consistent electrostatics. For example, at gate voltage $V_{\text{GS}} = 0.5$ V, due to the influence of band nonparabolicity, η_{FS} values for the two bandstructure models slightly differ [see dashed circle in Fig. 3(b)]. Comparing $I_{\text{DS}} - \eta_{\text{FS}}$ in Fig. 3(b) for the two models, however, confirms that current transport is well described by the parabolic EFM approximation for gate biases up to 0.5 V. It is also interesting to note that the maximum value of η_{FS} is about 120 meV in the device ON-state ($V_{\text{DS}} = V_{\text{GS}} = 0.5$ V), and the validity of the parabolic EFM model in

---

[1]In 1-D semiclassical transport, the device current is determine by the analytical expression $I_{\text{DS}} = (4q/h)k_BT\{\ln[1 + \exp(\eta_{\text{FS}}/k_BT)] - \ln[1 + \exp(\eta_{\text{FD}}/k_BT)]\}$ where $\eta_{\text{F,S(D)}} = E_{\text{F,S(D)}} - E_{\text{C-TOB}}$. Thus, I_{DS} is completely determined by the source/drain Fermi levels [$E_{\text{F,S(D)}}$] and top of channel barrier position [$E_{\text{C-TOB}}$].
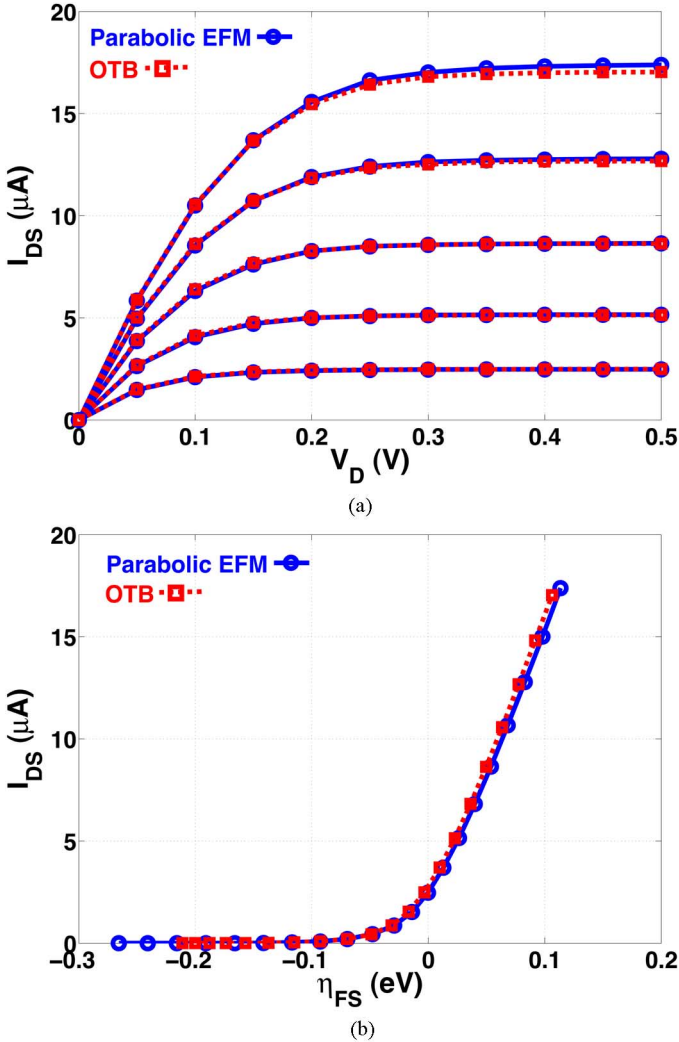
Fig. 4. *I–V* results for the (13,0) CNT MOSFET using NEGF simulation: solid circles—parabolic EFM and dashed squares—OTB. (a) $I_{DS} - V_{DS}$ for V_{GS} varied from 0.3 V to 0.5 V in steps of 0.05 V. (b) $I_{DS} - \eta_{FS}$ results with $V_{DS} = 0.5$ V and V_{GS} varied from 0.0 V to 0.5 V in steps of 0.025 V. (Color version available online at http://ieeexplore.ieee.org.)

this energy range is confirmed in Fig. 1. Consequently, the parabolic band approximation is indeed well suited for describing *I–V* characteristics of CNT MOSFETs in the bias ranges of practical interest.

As noted earlier, the device characteristics of CNT MOS-FETs explored above are simulated using the semiclassical BTE treatment. The BTE approach, however, does not capture any quantum transport effects such as tunneling and wavefunction interference. In order to examine the importance of such quantum effects and the possible influence of bandstructure models on quantum transport, we have performed NEGF simulations of the CNT MOSFET shown in Fig. 2 [15], [16]. For the case of the OTB model, the device is defined by the same nearest neighbor tight-binding Hamiltonian that has been employed in deriving (1) [15]. On the other hand, the EFM Hamiltonian is derived using the parabolic effective mass given by (2) [16]. The $I_{DS} - V_{DS}$ and $I_{DS} - \eta_{FS}$ results for the two transport simulations are shown in Fig. 4(a) and 4(b), respectively. From Fig. 4(a) it is evident that in the bias range of interest, the two bandstructure models give very similar output characteristics

even with quantum transport simulation, corroborating the previous results obtained from the semiclassical BTE transport. In Fig. 4(b), $I_{DS} - \eta_{FS}$ also agree very well for the two models and η_{FS} reaches a maximum value of only 110 meV, further supporting the validity of the parabolic band approximation.

By comparing the $I_{DS} - V_{DS}$ results from Fig. 3(a) with those of Fig. 4(a), it can be seen that the semiclassical BTE model persistently overestimates the output current compared to the NEGF results. Such discrepancy between semiclassical and quantum transport has been previously observed and can be understood by looking at the detailed nature of the charge induced in the channel region [20]. In the device ON-state, irrespective of the transport model, the total channel charge density is determined by the gate bias, $Q_{channel} = C_G(V_{GS} - V_T)$, where V_T is the threshold voltage. However, for the case of quantum transport, part of this channel charge resides below the conduction band edge due to quantum tunneling. Such carriers have a smaller velocity, thus reducing the total current for the quantum simulation compared to the semiclassical BTE calculation [20]. Nevertheless, the difference in the ON-current (at $V_{DS} = V_{GS} = 0.5$ V) determined by the two transport simulations is only ~10%. Another important quantum mechanical effect that can influence the OFF-current of the CNT MOSFET is due to band-to-band tunneling and the associated charge pile-up effect [4], [21]. For moderate drain biases and large bandgap CNTs, however, the effect of band-to-band tunneling is minimal. More importantly, with respect to the different bandstructure models, both semiclassical and quantum transport calculations confirm the validity of the parabolic effective mass approximation for CNT MOSFET simulation in voltage bias ranges of practical interest.

IV. CONCLUSION

Electronic dispersion of semiconducting zigzag CNTs has been studied using EHT, OTB, and the parabolic EFM. Using the former as the reference calculation, the empirical fitting parameter in the latter two models was determined and a better p_z relation was obtained. After proper calibration, the OTB and EHT band dispersions agree very well over a large energy range. The range of validity of the parabolic EFM for a (13,0) CNT MOSFET was examined using the semiclassical Boltzmann transport and NEGF quantum transport. It is found that both the transport simulations are consistent in their conclusions; that the parabolic effective mass approximation is a valid description of the electronic structure for practically applicable voltage bias conditions of CNT MOSFETs.

REFERENCES

[1] R. Tamura and M. Tsukada, "Analysis of quantum conductance of carbon nanotube junctions by the effective-mass approximations," *Phys. Rev. B*, vol. 58, pp. 8120–8124, Sep. 1998.

[2] H. Ajiki and T. Ando, "Electronic states of carbon nanotubes," *J. Phys. Soc. Jpn.*, vol. 62, pp. 1255–1266, Oct. 1992.

[3] D. L. John, L. C. Castro, P. J. S. Pereira, and D. L. Pulfrey, "A Schrodinger–Poisson solver for modeling carbon nanotube FETs," in *Proc. NSTI Nanotechnology*, 2004, vol. 3, pp. 65–68.

[4] J. Knoch, S. Mantl, and J. Appenzeller, "Comparison of transport properties in carbon nanotube field-effect transistors with Schottky contacts and doped source/drain contacts," *Solid-State Electron.*, vol. 49, pp. 73–76, 2005.

[5] G. Pennington and N. Goldsman, "Semiclassical transport and phonon scattering of electrons in semiconducting carbon nanotubes," *Phys. Rev. B*, vol. 68, p. 045426, 2003.

[6] J. Wang, E. Polizzi, and M. Lundstrom, "A three-dimensional quantum simulation of silicon nanowire transistors with the effective-mass approximation," *J. Appl. Phys.*, vol. 96, no. 4, pp. 2192–2203, Aug. 2004.

[7] M. Bescond, N. Cavassilas, K. Kalna, K. Nehari, L. Raymond, J. L. Autran, M. Lannoo, and A. Asenov, "Ballistic transport in Si, Ge, and GaAs nanowire MOSFETs," in *IEDM Tech. Digest*, 2005, pp. 533–536.

[8] P. Vogl, H. P. Hjalmarson, and J. D. Dow, "A semi-empirical tight-binding theory of the electronic structure of semiconductors," *J. Phys. Chem. Solids*, vol. 44, no. 5, pp. 365–378, 1983.

[9] T. B. Boykin, G. Klimeck, and F. Oyafuso, "Valence band effective-mass expressions in the $sp^3 d^5 s^*$ empirical tight-binding model applied to a Si and Ge parametrization," *Phys. Rev. B*, vol. 69, p. 115201, 2004.

[10] R. Saito, G. Dresselhaus, and M. S. Dresselhaus, *Physical Properties of Carbon Nanotubes*. London, U.K.: Imperial College Press, 2003.

[11] J. N. Murrell and A. J. Harget, *Semi-Empirical Self-Consistent Molecular Orbital Theory of Molecules*. New York: Wiley Interscience, 1972.

[12] D. Kienle, J. I. Cerda, and A. W. Ghosh, "Extended Hückel theory for electronic structure, chemistry and transport. I. Carbon nanotubes," *J. Appl. Phys.*, accepted for publication.

[13] J. Wang, A. Rahman, A. Ghosh, G. Klimeck, and M. Lundstrom, "On the validity of the parabolic effective-mass approximation for the *I–V* calculation of silicon nanowire transistors," *IEEE Trans. Electron Devices*, vol. 52, no. 7, pp. 1589–1595, Jul. 2005.

[14] J.-H. Rhew, Z. Ren, and M. S. Lundstrom, "A numerical study of ballistic transport in a nanoscale MOSFET," *Solid-State Electron.*, vol. 46, pp. 1899–1906, 2002.

[15] J. Guo, S. Datta, M. Lundstrom, and M. P. Anantram, "Multi-scale modeling of carbon-nanotube transistors," *Int. J. Multiscale Comp. Eng.*, vol. 2, p. 257, 2004.

[16] S. Datta, "Nanoscale device modeling: The Green's function method," *Superlattices Microstruct.*, vol. 28, no. 4, pp. 253–278, 2000.

[17] J. C. Slater and G. F. Koster, "Simplified LCAO method for the periodic potential problem," *Phys. Rev.*, vol. 94, pp. 1498–1524, Jun. 1954.

[18] Jorge Iribas Cerda home page [Online]. Available: www.icmm.csic.es/jcerda/index.html

[19] J. W. G. Wildoer, L. C. Venema, A. G. Rinzler, R. E. Smalley, and C. Dekker, "Electronic structure of atomically resolved carbon nanotubes," *Nature*, vol. 391, no. 1, pp. 59–62, Jan. 1998.

[20] Z. Ren, R. Venugopal, S. Datta, and M. Lundstrom, "The ballistic nanotransistor: a simulation study," in *IEDM Tech. Digest*, 2000, pp. 715–718.

[21] G. Fiori, G. Iannaccone, and G. Klimeck, "Performance of carbon nanotube field effect transistors with doped source and drain extensions and arbitrary geometry," in *IEDM Tech. Digest*, 2005, pp. 529–532.

Siyuranga Koswatta received the B.S in computer engineering (*summa cum laude*) from the University of Bridgeport, Bridgeport, CT in 2002 and the M.S.E.C.E. degree from Purdue University, West Lafayette, IN, in 2004. He is currently working toward the Ph.D. degree in electrical and computer engineering at Purdue University.

His research interests are mainly in quantum transport and nanoscale device modeling. He has been exploring novel applications and device physics for carbon nanotube transistors.

Neophytos Neophytou (S'03) received the B. S. degree in electrical and computer engineering and the M.S. degree in microelectronics and nanotechnology from Purdue University, West Lafayette IN in 2001 and 2003, respectively. He is currently working toward the Ph.D. degree at Purdue University.

His research interests include computational modeling of electron transport through carbon nanotubes and III–V materials. He is currently working on the effects of bandstructure on the electronic properties of different materials and the effect of the three-dimensional electrostatic environment on the electronic transport through nanoscale devices.

Diego Kienle received the Diploma degree (M.S.) in theoretical physics from the University of Bayreuth, Germany, in 1997, working on dynamical correlation functions of one-dimensional Luttinger liquids. He received the Ph.D. in theoretical physics from the University of Saarland, Germany, in 2001, working in the Research Center Juelich, Germany, on modeling and simulation of complex polymer fluids by means of Brownian dynamics (BD) with emphasis on polymer-flow interaction.

He was a Research Assistant with the University of Saarland until December 2002. From February 2003 to February 2006, he was a Postdoctoral Research Associate in the group of Prof. M. Lundstrom, working on modeling of the electronic structure of nanostructures, computational modeling of quantum transport simulations, and nonorthogonal tight-binding parametrizations with improved transferability. He is currently with Purdue University, West Lafayette, IN. His research interests are empirical modeling of electronic structure of nanostructures using nonorthogonal tight-binding, quantum transport simulation through molecules and nanotubes using the nonequilibrium Green function, modeling of complex fluids using Brownian dynamics, and hydrodynamic interaction in polymer systems.

Gianluca Fiori received the degree in electronic engineering and the Ph.D. degree from the Università di Pisa, Pisa, Italy, in 2001 and 2005, respectively.

In autumn 2002, he was in SILVACO International developing quantum models, which are corrently implemented in the ATLAS simulator. In summer 2004 and 2005, he was with Purdue University, West Lafayette, IN, working on models for the simulation of transport in nanoscaled devices. He is currently with the Dipartimento di Ingegneria dell'Informazione, Università di Pisa, holding a postdoctoral position. His main field of research activity is the development of models and codes for the simulations of ultrascaled semiconductor devices.

Mark S. Lundstrom (S'74–M'78–SM'80–F'94) received the B.E.E. and M.S.E.E. degrees from the University of Minnesota, Minneapolis, in 1973 and 1974, respectively, and the Ph.D. degree in electrical engineering from Purdue University, West Lafayette, IN in 1980.

From 1974 to 1977, he worked at Hewlett-Packard Corporation, Loveland, CO, on integrated circuit process development and manufacturing support. In 1980, he joined the School of Electrical Engineering, Purdue University, where he is currently the Don and Carol Scifres Distinguished Professor of Electrical and Computer Engineering and the Founding Director of the Network for Computational Nanotechnology. From 1989 to 1993, he was Director of Purdue University's Optoelectronics Research Center, and from 1991 to 1994, he was Assistant Dean of Engineering. His research interests center on carrier transport in semiconductors and the physics of small electronic devices, especially nanoscale transistors.

Prof. Lundstrom currently serves as an IEEE Electron Device Society Distinguished Lecturer. He is a Fellow of the American Physical Society. In 1992 he received the Frederick Emmons Terman Award from the American Society for Engineering Education. With his colleague, S. Datta, he was awarded the 2002 IEEE Cledo Brunetti award for their work on nanoscale electronic devices. In the same year they shared the Semiconductor Research Corporation's Technical Excellence Award. In 2005, he received the Semiconductor Industry Association's University Researcher Award for his career contributions to the physics and simulation of semiconductor devices.